Project 2

3-D Euler-Bernoulli Beam Analysis on a Rocket

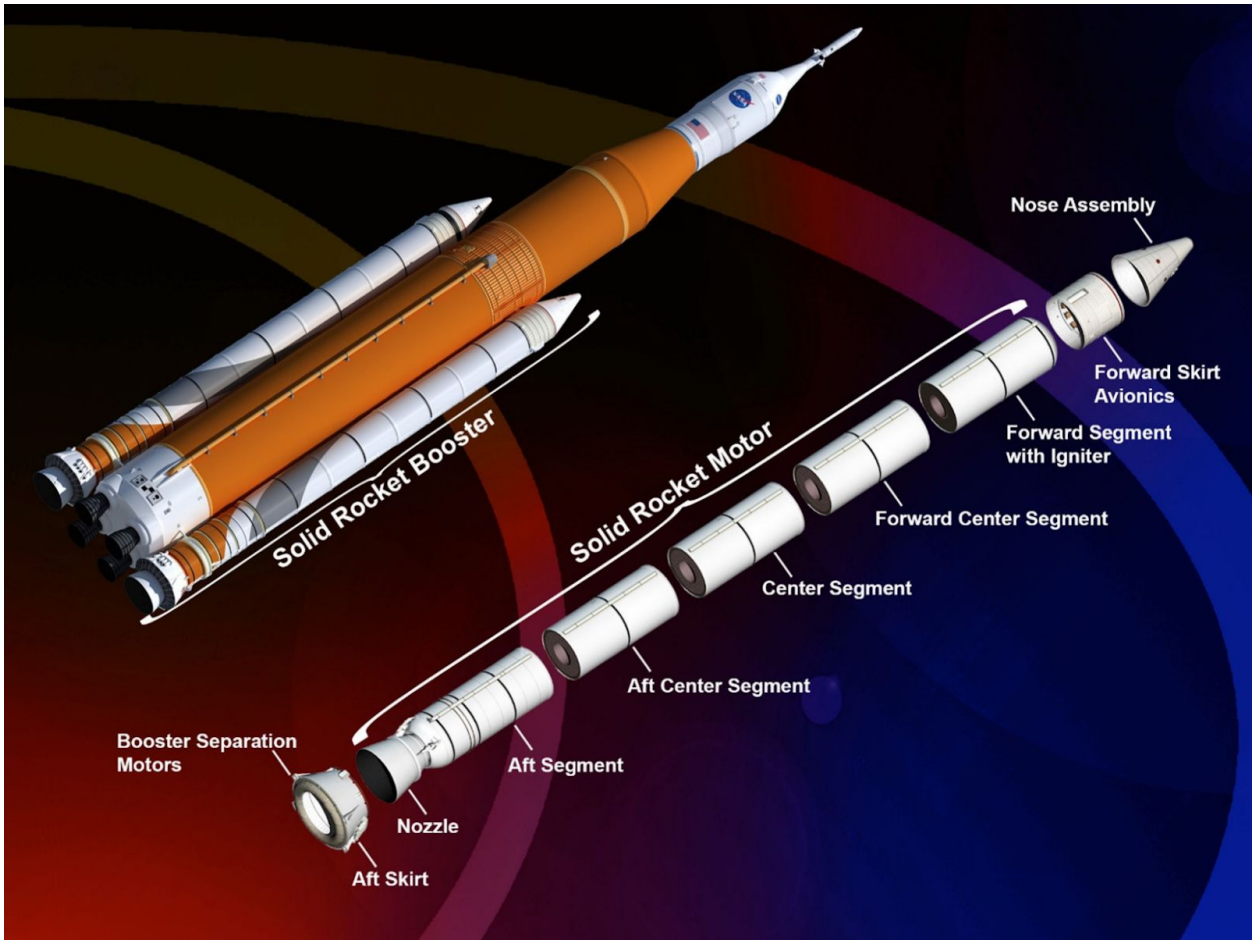

Emre Mengi and Zachary Price

02.21.2020

EAE 135

ABSTRACT

This report delves into a preliminary structural analysis of a rocket motor section using the Euler-Bernoulli beam method under simplified conditions. A casing made of eight laminated layers of carbon epoxy is scrutinized under loading from thrust vectoring and the axial and transverse displacements of this casing are calculated. The maximum stresses in each layer are deduced and are found to have a high chance of survival under the preset conditions and offer a more lightweight model than a typical aluminum casing. It was concluded that the carbon epoxy casing provides a solid structural housing for the rocket under the specified assumptions, but a more in-depth analysis must be done in order to approve the design for flight.

INTRODUCTION

As in the previous project, a rocket's structure is analyzed during equilibrium. This report delves into a slightly more in-depth analysis of the rocket while undergoing thrust vectoring at a maximum gimbal deflection angle. Thrust vectoring makes the rocket more versatile and allows for additional control during flight. This thrust vectoring induces transverse loads and bending moments in addition to the initial axial loading. The motor is analyzed by assuming it is one homogenous segment, thrust is a point-force, dynamic effects and buckling are neglected, the weight of the motor is a distributed transverse load, and the loss of weight due to fuel is neglected. The solid propellant, HTPB, is aged 12 days and the roller, wall, and ground are rigid bodies. The rocket casing that is under scrutiny is made of eight layers of equal thickness of AS4/3501-6 carbon/epoxy. This material, also known as black aluminum, surrounds the inner diameter of the rocket which holds the solid propellant and is manufactured with a [0,±45,90] symmetric configuration.

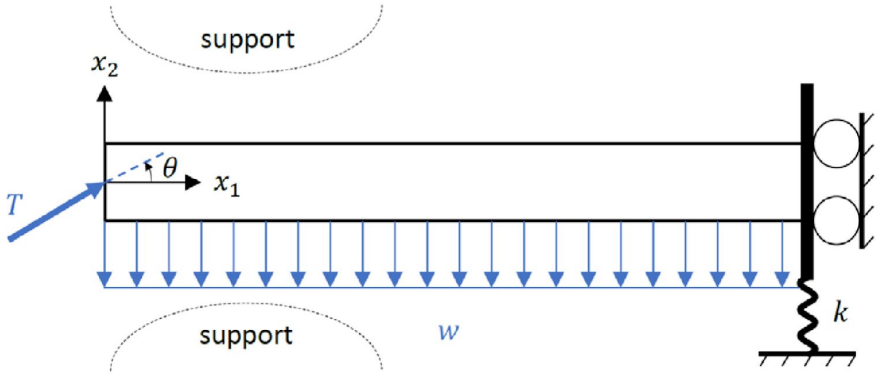

Figure 1: Simplified Model for the Rocket Motor

The structural analysis of this motor uses a 3D Euler-Bernoulli beam theory with the assumption that the rocket is a long, thin beam in equilibrium. The first step is to find the different boundary conditions for the beam which will be used to find the axial and transverse loads. Next, the fundamentals of composite mechanics will be used to calculate the reduced stiffness matrix which will determine the axial and transverse displacements. The maximum tensile and compressive stresses in each layer will then be calculated and defined as critical point locations, or locations where the beam is most likely to fail. Taking these critical point values and the safety and fitting factors, each layer will be determined to either fail or survive the applied loads and moments.

METHODS

The deliverables requested are as follows:

- Maximum deflection angle, ,
- Boundary conditions required to obtain axial and transverse displacement distributions of the beam centerline,
- Axial displacement, u_1, and transverse displacement, u_2,
- Moment about x_3 along the length of the beam,
- Axial position where stress in the layers is maximum,
- Axial stress distribution, $_1$, along x_2 in x_1x_2 plane,
- Evaluation of a possible casing failure given the safety and fitting factors.

First, a force balance for x_2 direction and moment about the centroid of the motor can be written, in order to obtain the maximum deflection angle of the thrust:

Force balance:

$$\sum F_{x_2} = 0$$

$$T * sin\theta + F_s - wL = 0$$

Moment balance:

$$M_o = -T * sin\theta * \frac{L}{2} + F_s * \frac{L}{2} = 0$$

$$F_s = Tsin\theta$$

Plugging this result back into the force balance will yield:

$$\theta = \sin^{-1}\left(\frac{wL}{2T}\right)$$

Next, the boundary conditions must be set, in order to solve the differential equations that yields the displacement distributions in axial and transverse directions.

Boundary conditions required to obtain the axial displacement are:

For x_1=0, the external force, the thrust vector, is equal to the internal force, N_1:

$$-N_1(0) = Tcos\theta$$

For x_1=L, the motor is fixed due to the roller support on the right, meaning there would be no displacement in the axial direction:

$$u_1(L) = 0$$

Now, the internal force can be solved by integrating the following relation:

$$\frac{dN_1}{dx_1} = -P_1$$

which yields:

$$N_1 = -P_1 x + C_1$$

As there is no load distribution in the axial direction, P_1 is equal to zero. C_1 can be obtained by using the boundary condition defined above:

$$N_1 = -Tcos\theta$$

The axial displacement distribution is:

$$\frac{du_1}{dx_1} = \frac{N_1}{S}$$

After integration and applying the displacement boundary condition, the axial displacement distribution is obtained:

$$u_1(x_1) = \frac{Tcos\theta}{S}(L - x_1)$$

Boundary conditions required to obtain the transverse displacement are:

For x_1=0, the bending moment vanishes due to the free end:

$$M_3(0) = H_{33}^c \frac{d^2u_2(0)}{dx_1^2} = 0$$

Also, the internal force at x_1=0, the shear force, is equal to the external transverse thrust vector:

$$\frac{dM_3(0)}{dx_1} = -\left(-\frac{d}{dx_1}\left[H_{33}^c \frac{d^2u_2}{dx_1^2}\right]\right) = Tsin\theta$$

For x_1=L, the vertical equilibrium of forces at the location of the spring force yields:

$$\frac{d}{dx_1}\left[H_{33}^c \frac{d^2u_2}{dx_1^2}\right] - ku_2(L) = 0$$

In addition, the following conditions applies due to the roller support on the right end of the motor:

$$\frac{du_2(L)}{dx_1} = 0$$

Using these four boundary conditions, the transverse displacement can be solved by integrating the following expression 4 times:

$$\frac{d^2}{dx_1^2}\left[H_{33}^c \frac{d^2u_2}{dx_1^2}\right] = p_2(x_1)$$

First integration results in:

$$\frac{d}{dx_1}\left[H_{33}^c \frac{d^2u_2}{dx_1^2}\right] = P_2x_1 + C_1$$

which can be solved by using the force boundary condition at the left end of the motor:

$$\frac{d}{dx_1}\left[H_{33}^c \frac{d^2u_2}{dx_1^2}\right] = P_2x_1 + Tsin\theta$$

Now, the spring force boundary condition at the right end of the motor can be used to obtain a displacement boundary condition:

$$\frac{d}{dx_1}\left[H_{33}^c \frac{d^2u_2}{dx_1^2}\right] = ku_2(L)$$

Using the last two relations, a BC at x_1=L for u_2:

$$u_2(L) = \frac{P_2L}{k} + \frac{Tsin\theta}{k}$$

This boundary condition will be used later in order to obtain the final form of the

transverse displacement distribution.

Next, the third order differential equation is integrated and the moment boundary condition at at left end of the motor is applied:

$$H_{33}^{c}\frac{d^2u_2}{dx_1^2} = P_2x_1^2 + Tsin\theta * x_1$$

This expression is then integrated again and another boundary condition is applied:

$$\frac{du_2}{dx_1} = \frac{P_2x_1^3}{6H_{33}^{c}} + \frac{Tsin\theta}{2H_{33}^{c}}x_1^2 + C_3 \qquad \frac{du_2(L)}{dx_1} = 0$$

,

Then,

$$\frac{du_2}{dx_1} = \frac{P_2}{6H_{33}^{c}}(x_1^3 - L^3) + \frac{Tsin\theta}{2H_{33}^{c}}(x_1^2 - L^2)$$

Finally, this expression is integrated once more and the previously obtained boundary condition for $u_2(L)$ is used:

$$u_2(x_1) = \frac{P_2}{24H_{33}^{c}}x_1^4 + \frac{Tsin\theta}{6H_{33}^{c}}x_1^3 + \left(-\frac{P_2}{6H_{33}^{c}}L^3 - \frac{Tsin\theta}{2H_{33}^{c}}L^3\right)x_1 + \frac{P_2L^4}{8H_{33}^{c}} + \frac{Tsin\theta}{3H_{33}^{c}}L^3 + \frac{P_2L}{k} + \frac{Tsin\theta}{k}$$

In order to numerically calculate the axial and transverse displacement distributions, axial stiffness (S) and bending stiffness (H_{33}) need to be calculated. Because the casing is made of multiple layers that have different orientations, these values need to be calculated using the lamination plate theory. These steps can be found in the notes about bending stiffness of a laminated beam (La Saponara, 1-4)

First, the reduced stiffness matrix, Q, is calculated:

$$Q = \begin{bmatrix} \frac{E_{11}}{1-\nu_{12}\nu_{21}} & \frac{\nu_{21}E_{11}}{1-\nu_{12}\nu_{21}} & 0 \\ \frac{\nu_{12}E_{22}}{1-\nu_{12}\nu_{21}} & \frac{E_{22}}{1-\nu_{12}\nu_{21}} & 0 \\ 0 & 0 & G_{12} \end{bmatrix} \quad \text{where } \nu_{21} = \nu_{12}\, E_{22}/E_{11}$$

The values for the Young Modulus and Poisson's ratio for different directions are obtained from the table with composite material properties, which is included below:

Table 1. Composite properties for AS4/epoxy. From: Swanson, S.R. *Introduction to Design and Analysis with Advanced Composite Materials*. 1997.Herakovich, C.T. *Mechanics of Fibrous Composites*. 1997.

Material	AS4/Epoxy
E_{11} [GPa]	148.24
E_{22} [GPa]	10.07
12	0.30
G_{12} [GPa]	4.58

Then, the Qbar is calculated:

$$\overline{Q} = T^{-1} \cdot Q \cdot R \cdot T \cdot R^{-1}$$

where T and R matrices are as follows:

$$T = \begin{bmatrix} \cos^2\beta & \sin^2\beta & 2\sin\beta\cos\beta \\ \sin^2\beta & \cos^2\beta & -2\sin\beta\cos\beta \\ -\sin\beta\cos\beta & \sin\beta\cos\beta & \cos^2\beta - \sin^2\beta \end{bmatrix}, \quad R = \begin{bmatrix} 1 & 0 & 0 \\ 0 & 1 & 0 \\ 0 & 0 & 2 \end{bmatrix}$$

The Qbar found is then inverted to obtain Sbar, whose element in the first row and first column is the reciprocal of the Young's Modulus of the laminate layer:

$$\left(E_{x1x1}\right)_{ith} = \frac{1}{\left(\bar{S}_{11}\right)_{ith}}$$

This process is reiterated for each laminate layer to obtain the Young's Modulus values.

Next, axial stiffness can be found by the following formula:

$$S = \int_A E dA = \sum_{i=1}^{8} E_i * A_i$$

where the area defined is the individual areas of the layers and E is the Young's Modulus of individual layers.

Bending stiffness of the laminate can be calculated by using the relation:

$$H_{33}^c = \iint E x_2^2 \, dA = \sum_{i=1}^{n} \int_0^{2\pi} \int_{r_i}^{r_{i+1}} E\left(r\sin\theta\right)^2 r \, dr \, d\theta$$

After evaluating this integral, the following relation is found and used in the bending stiffness calculation:

$$H_{33}^c = \frac{\pi}{64} \sum_{i=1}^{8} E_i (D_{i+1}^4 - D_i^4)$$

After calculating the displacement distributions, the moment along the length of the motor is calculated with the following relation:

$$M_3(x_1) = H_{33}^c \frac{d^2 u_2}{dx_1^2} = P_2 x_1^2 + T sin\theta * x_1$$

The critical location in x_1 in terms of maximum axial stresses in the layers can be found by finding the location of the maximum bending moment. The axial stress due to the axial load does not vary along the length, so the critical location is only dependent on the moment.

At the critical axial location, x_{cr} , the axial stress along x_2 in the cross-section can be found by summing up the axial stresses due to bending and axial loading:

$$\sigma_{total} = \sigma_{bending} + \sigma_{axial}$$

Axial stress was calculated through the following relation:

$$\sigma_{axial} = E * \frac{N_1}{S}$$

This calculation was performed for the laminate layers and the propellant with each respective Young's Modulus value.

Bending stress was calculated using the following, which was also reiterated for each layer, at the outer radius, in order to capture the maximum stress in each layer:

$$\sigma_{bending} = -E * \frac{\frac{D}{2} * M_{3,max}}{H_{33}^c}$$

After plotting the total axial stress on the cross-section at the critical location, the maximum stress values were adjusted according to the given safety and fitting factors in the following manner:

$$FOS = s_f * f_f$$

By comparing the adjusted stress values to the given tensile and compressive strengths in axial and transverse directions, the casing was evaluated for a possible failure. The strength values used are tabulated below:

Table 2. Propellant parameters. From: Swanson, S.R. *Introduction to Design and Analysis with Advanced Composite Materials*. 1997, Herakovich, C.T. *Mechanics of Fibrous Composites*. 1997.

Material	AS4/Epoxy
Axial Tensile Strength [MPa]	2137.37
Transverse Tensile Strength [MPa]	53.43
Axial Compressive Strength [MPa]	-1268.64
Transverse Compressive Strength [MPa]	-168.23

In addition, the following rocket and motor properties were used in order to numerically analyze the structure:

Table 3. Rocket and motor parameters. From: La Saponara, Valeria. *EAE 135 - Aerospace Structures, Project 2 Handout*. 19 February 2020.

Outer diameter: 3.71 m	Casing thickness: 120 mm
Length: 46 m	Thrust: 1578 tf
Single layer thickness: of casing thickness	Motor weight: $1.825 * 10^5$ N/m
Spring constant: 10^8 kN/m	HTPB propellant density: 1750 $kg/\boldsymbol{m}^3$
HTPB propellant elastic modulus: 4.86 MPa	

Using this methodology, the deliverables were calculated and presented in the following section.

RESULTS

The maximum deflection angle ( ) calculated is:

$$\theta = 15.74°$$

Next, in order to calculate the numerical values of the displacement distributions, the Young's Modulus values for each layer was obtained through classical laminate plate theory:

Table 4. Layer Young's Modulus values.

Layer Orientation	Young Modulus (E) [GPa]
0°	148.24
45°	14.23
-45°	14.23
90°	10.07

Axial and transverse displacement distributions obtained through the relations calculated in the previous section are plotted along the length of the rocket:

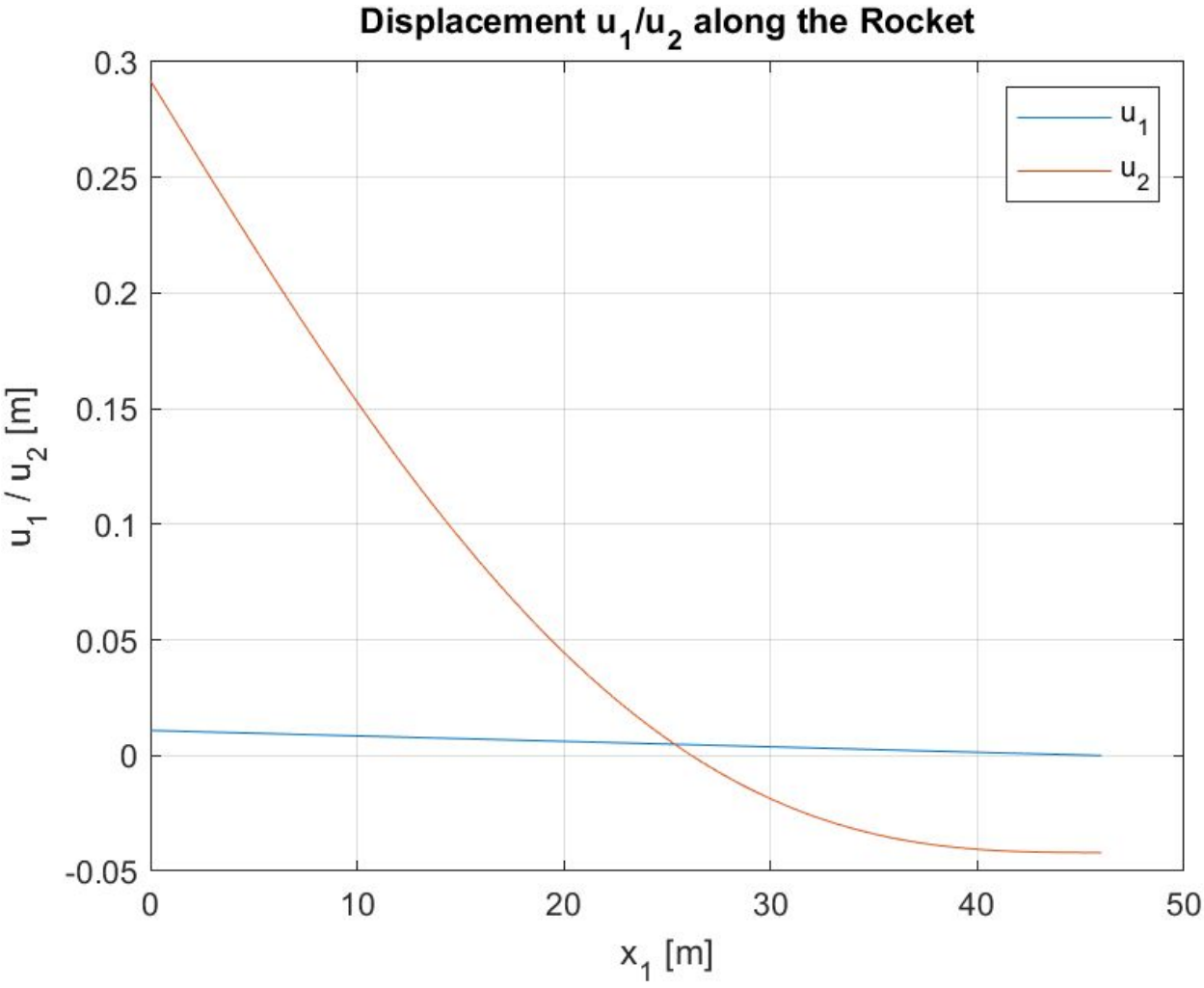

Figure 2: Axial and transverse displacement distribution along the rocket.

After calculating the displacement distributions, the moment distribution along the rocket is additionally calculated and plotted:

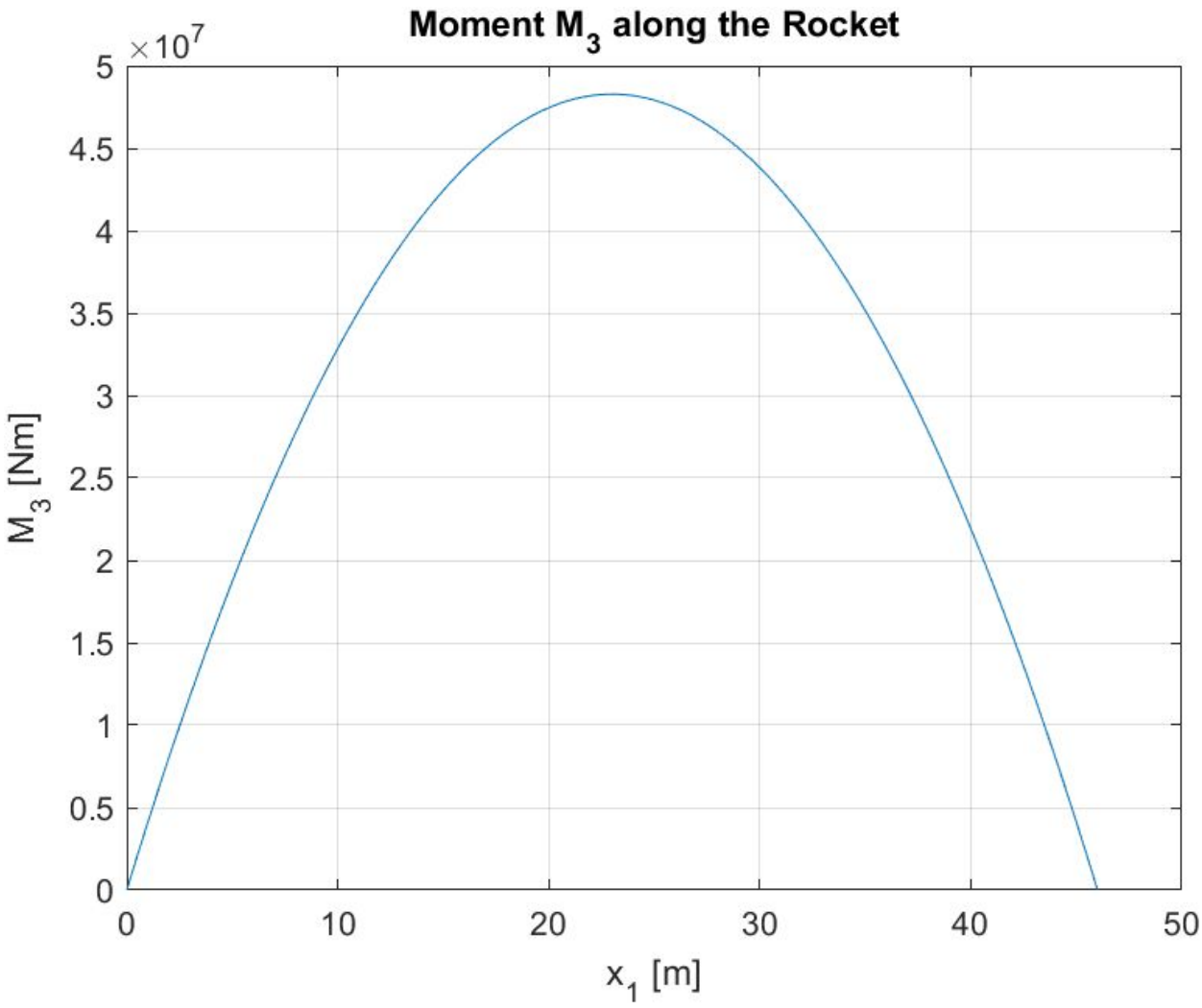

Figure 3: Moment (M_3) distribution along the rocket.

The critical axial location, x_{cr}, where the axial stresses are the maximum along the cross-section of the motor is at the point where the moment is maximum. The axial stress due to the axial load is constant along the length of the motor, therefore, does not have an effect on the location of the critical axial location. Thus, x_{cr} is calculated to be at:

$$x_{cr} = 23.02\ m$$

At this critical x_1 location, the axial stresses due to bending and axial loading were calculated along the radius of the motor and presented below:

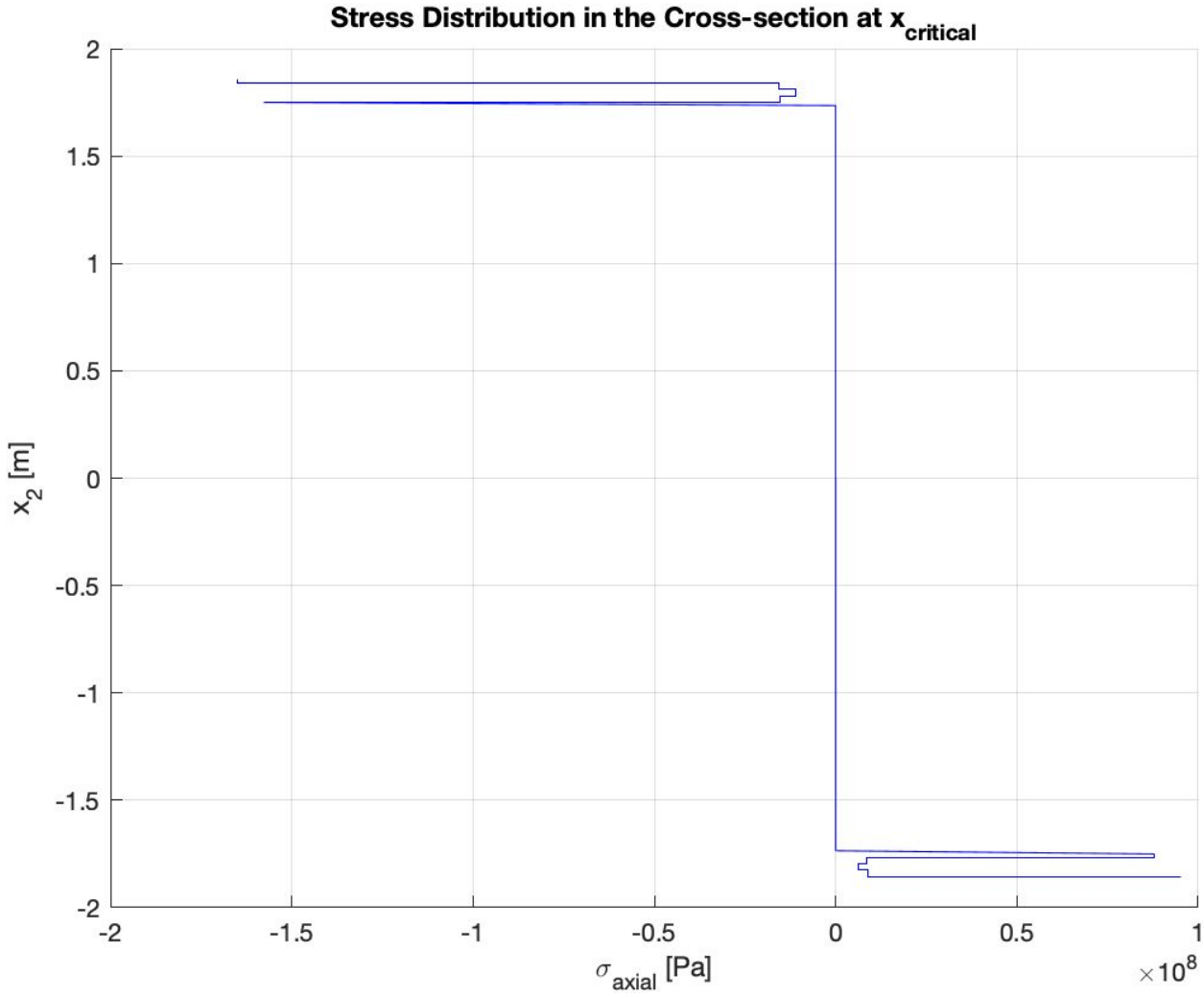

Figure 4: Stress distribution in the cross-section at x_{cr}.

The sections on the graph where the laminate are can be zoomed in, in order to closely analyze the effect of the loading on the casing structure:

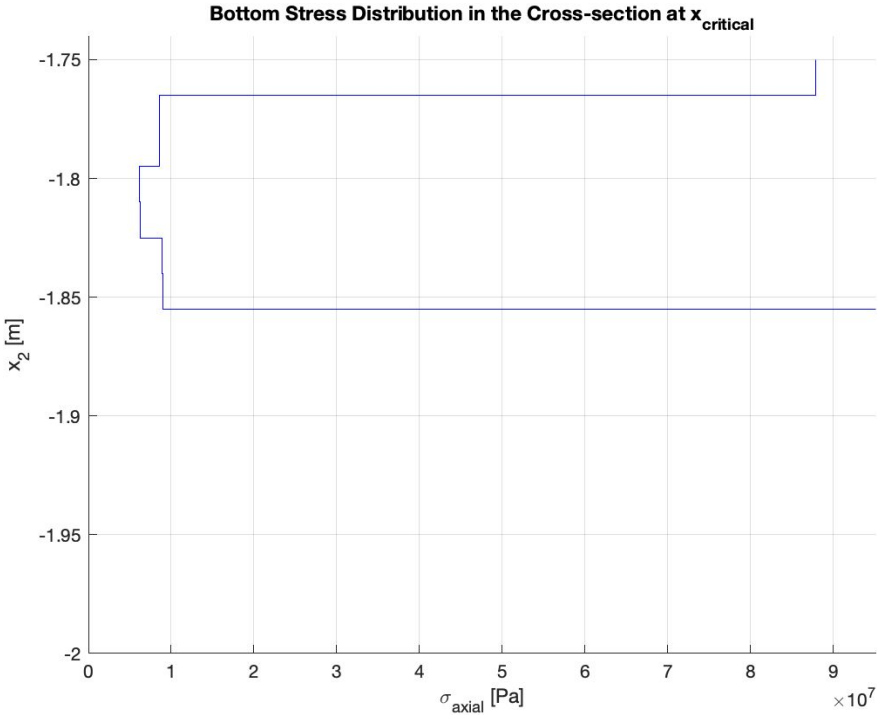

Figure 5: Stress distribution in the cross-section at the lower laminate section at x_{cr}.

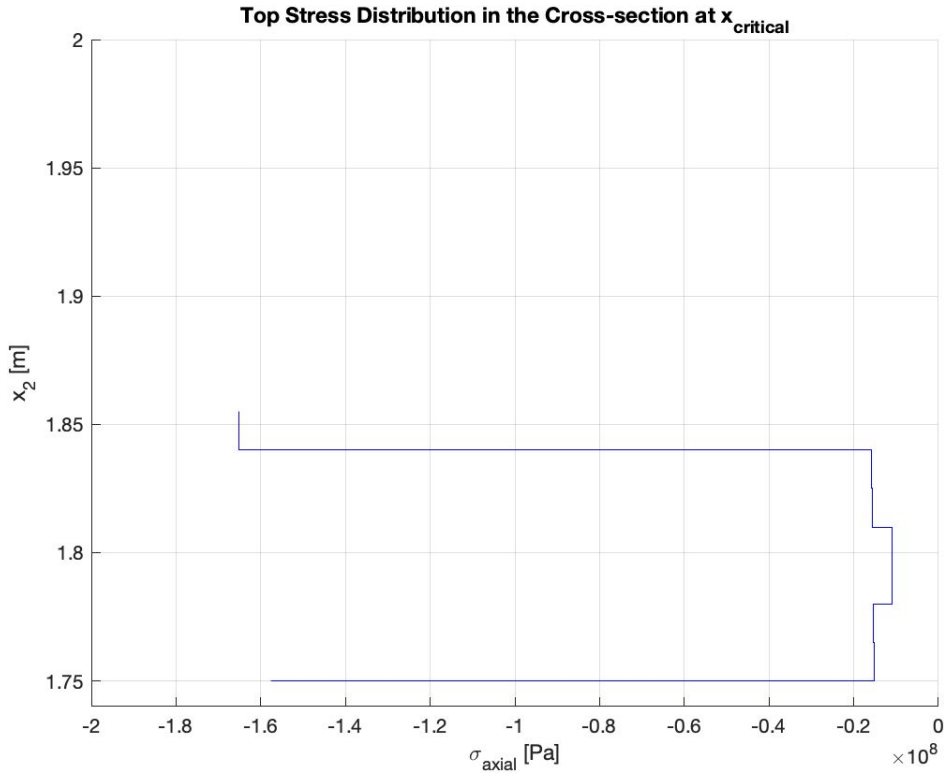

Figure 6: Stress distribution in the cross-section at the upper laminate section at x_{cr}.

The maximum stresses with their adjusted values are presented along with the corresponding yield strengths for each layer of the casing for failure evaluation:

Table 5. Maximum stress values for different layers of the composite casing.

Material	Orientation	Maximum Stress, $_{max}$ [MPa]	Maximum Stress by FOS, $_{allow}$ [MPa]	Yield Strength of AS4, $_{Y.S.}$ [MPa]	Risk of Failure
Layer 1 (0°)	Top	-157.69	-226.68	-1268.64	No
	Bottom	95.2	136.84	2137.37	No
Layer 2 (45°)	Top	-15.24	-21.91	-168.23	No
	Bottom	9.04	12.99	53.43	No
Layer 3 (-45°)	Top	-15.34	-22.05	-168.23	No
	Bottom	8.94	12.85	53.43	No
Layer 4 (90°)	Top	-10.92	-15.70	-168.23	No
	Bottom	6.25	8.98	53.43	No
Layer 5 (90°)	Top	-10.99	-15.80	-168.23	No
	Bottom	6.18	8.88	53.43	No
Layer 6 (-45°)	Top	-15.64	-22.49	-168.23	No
	Bottom	8.63	12.41	53.43	No
Layer 7 (45°)	Top	-15.74	-22.63	-168.23	No
	Bottom	8.53	12.26	53.43	No
Layer 8 (0°)	Top	-165.06	-237.27	-1268.64	No
	Bottom	87.83	126.25	2137.37	No

DISCUSSIONS

The maximum deflection angle, , is caused by the thrust vectoring of the rocket and is considered the angle that results in static equilibrium, which is the set-up that the rest of the report builds off of. This maximum deflection angle is found to be 15.74° and is a function of the thrust, weight, and length of the rocket.

For a laminated beam with a cylindrical cross-section, the centroidal bending stiffness, H_{33}^{c}, is calculated to be $1.0203 \times 10^{11} N \bar{A} m^2$ and the axial stiffness, S, is calculated to be $6.3194 \times 10^{10} N$ which will be used to find u_2 and u_1, respectively. The axial and transverse displacements are plotted in Figure 2 against the length of the rocket. The transverse displacement is found to be much larger than the axial displacement along the beam, reaching a maximum of 0.3 meters at x = 0 and a minimum of -0.04 meters at x= L. The distribution of the bending moment is also shown in Figure 3 and indicates that the maximum bending moment is located at 23.02 meters, also known as the critical axial position. Because the axial stress due to axial loading is constant along the beam, only the bending moment affects the critical axial position.

Figure 4 plots the total axial stress against x_2 at the location of maximum stress, $x_{critical}$. It can be seen that the propellant does not undergo a significant amount of axial stress compared to the laminated layers. Figure 4 also shows that the top of the rocket will be in compression and the bottom will be in tension, indicated by the negative and positive stress values, respectively. The plot is slightly asymmetric which is due to the constant axial loading that is added to both the compression and tension values, creating a slight offset. Figures 5 and 6 show the laminated layers of the rocket casing in response to the applied loads from the thrust vectoring. It is seen that the 0° laminated layer can withstand the largest amount of stress, while the 90° layers can withstand the least.

The culmination of this report is summarized in Table 5. Each layer's maximum calculated stress for both tension and compression is reported and compared with their maximum yield stress values to determine failure in the beam. As seen in the table, every layer survives the applied loads in both compression and tension with a large margin of safety. The layers in compression undergo a larger overall stress load, with the maximum stress at the outer layers and the minimum stress at the axis of symmetry. Thus reinforcing the importance of having the 0° laminated layers on the outermost section of the beam to withstand the highest stress values. The composite structure of this rocket casing will easily survive equilibrium flight during the stated conditions, but

will also be significantly lighter than an aluminum casing. Before approving such a casing design, further analysis must be done for all types of flight and without the generalizing assumptions that were made in this report, however, this report has proved that the rocket will survive under the specified conditions.

CONCLUSIONS

This report has successfully analyzed a rocket's structural integrity while undergoing thrust vectoring using the 3D Euler-Bernoulli beam theory under simplifying conditions. By finding the axial and transverse displacements, the stresses in each layer of the rocket casing were calculated and analyzed at the x_1 location of maximum axial stress. The composite rocket casing was found to survive the flight condition with a large margin of safety, however, a more in-depth study should be completed before this casing design is approved for flight.

REFERENCES

La Saponara, Valeria. *EAE 135 - Aerospace Structures, Project 2 Handout.* 19 February 2020.

La Saponara, Valeria. *EAE 135 - Aerospace Structures, Bending Stiffness of a Laminated Beam.* 11 February 2020.

Gligorijevic, Nikola et al. (2014). *Mechanical Properties of HTPB Composite Propellants in the Initial Period of Service Life*. Sci. Tech. Rev.. 64. 2-11.

Swanson, S.R. *Introduction to Design and Analysis with Advanced Composite Materials.* 1997.

Herakovich, C.T. *Mechanics of Fibrous Composites*. 1997.

Bauchau, Olivier Andre, and J. I. Craig. *Structural Analysis with Applications to Aerospace Structures*. Springer, 2009.

APPENDICES

Appendix A. MATLAB Code

```
%% Project 2
%Emre Mengi and Zachary Price

clc; clear all; close all; % housekeeping
%Part 1
W = 1.825 * 10^5; %N/m
L = 46; %meters
T = 1578 * 9.805 * 10^3; %Newtons
theta = asin((W*L)/(2*T));
theta_deg = 180 * theta / pi;
```

```
%% Part 2
t_c = 0.12; %casing thickness [m]
t_layer = t_c / 8; %single layer thickness
E_p = 4.86 * 10 ^6; %propellant elastic modulus in Pa
k = 10^8; %spring constant in N/m

D_o = 3.71; %outer diameter [m]
g = 9.805; %gravitational acceleration [m/s^2]
d_p = 1750; %HTPB propellant density [kg/m^3]

d_c = 0.055 * 1/2.205 * (39.37)^3; %casing density [kg/m^3]
A_p = pi/4 * (D_o - 2*t_c)^2;
A_c = pi/4 * (D_o^2 - (D_o - 2*t_c)^2);
P_2 = (-1) * g * (d_p * pi/4 * (D_o - 2*t_c)^2 + d_c * pi/4 * (D_o^2 - (D_o - 2*t_c)^2));

N_1 = -1 * T * cos(theta);
E_11 = (21.5*10^6) *6895; %Pa
E_22 = (1.46*10^6)*6895; %Pa
nu_12 = 0.3;
G_12 = (0.81 * 10^6) * 6895; %Pa
nu_21 = (E_22 / E_11) * nu_12;

% finding E
Q = [E_11/(1-nu_12*nu_21), E_11*nu_21/(1-nu_12*nu_21), 0;E_22*nu_12/(1-nu_12*nu_21), E_22/(1-nu_12*nu_21), 0;0, 0, G_12];
R = [1 0 0;0 1 0;0 0 2];
% calculating T
% 0 degrees
beta_0 = 0;
T_0 = [(cosd(beta_0))^2 (sind(beta_0))^2 2*sind(beta_0)*cosd(beta_0);
    (sind(beta_0))^2 (cosd(beta_0))^2 -2*sind(beta_0)*cosd(beta_0);
    -1*sind(beta_0)*cosd(beta_0) sind(beta_0)*cosd(beta_0) ((cosd(beta_0))^2)-((sind(beta_0))^2)];
Q_0_b = inv(T_0)*Q*R*T_0*inv(R);
S_0_b = inv(Q_0_b);
E_0 = 1/S_0_b(1,1);
% 90 degrees
beta_90 = 90;
T_90 = [(cosd(beta_90))^2 (sind(beta_90))^2 2*sind(beta_90)*cosd(beta_90);
    (sind(beta_90))^2 (cosd(beta_90))^2 -2*sind(beta_90)*cosd(beta_90);
    -1*sind(beta_90)*cosd(beta_90) sind(beta_90)*cosd(beta_90) ((cosd(beta_90))^2)-((sind(beta_90))^2)];
Q_90_b = inv(T_90)*Q*R*T_90*inv(R);
```

```
S_90_b = inv(Q_90_b);
E_90 = 1/S_90_b(1,1);
% 45 degrees
beta_45 = 45;
T_45 = [(cosd(beta_45))^2 (sind(beta_45))^2 2*sind(beta_45)*cosd(beta_45);
    (sind(beta_45))^2 (cosd(beta_45))^2 -2*sind(beta_45)*cosd(beta_45);
    -1*sind(beta_45)*cosd(beta_45) sind(beta_45)*cosd(beta_45) ((cosd(beta_45))^2)-((sind(beta_45))^2)];
Q_45_b = inv(T_45)*Q*R*T_45*inv(R);
S_45_b = inv(Q_45_b);
E_45 = 1/S_45_b(1,1);
% -45 degrees
beta_m45 = -45;
T_m45 = [(cosd(beta_m45))^2 (sind(beta_m45))^2 2*sind(beta_m45)*cosd(beta_m45);
    (sind(beta_m45))^2 (cosd(beta_m45))^2 -2*sind(beta_m45)*cosd(beta_m45);
    -1*sind(beta_m45)*cosd(beta_m45) sind(beta_m45)*cosd(beta_m45) ((cosd(beta_m45))^2)-((sind(beta_m45))^2)];
Q_m45_b = inv(T_m45)*Q*R*T_m45*inv(R);
S_m45_b = inv(Q_m45_b);
E_m45 = 1/S_m45_b(1,1);

E_lam = [E_0,E_45,E_m45,E_90,E_90,E_m45,E_45,E_0]; %youngs moduli for the casing sections
% calculating S
A_0_o = pi/4 * ((D_o - 0*t_c)^2 - (D_o - 1/4*t_c)^2);
A_45_o = pi/4 * ((D_o - 1/4*t_c)^2 - (D_o - 2/4*t_c)^2);
A_m45_o = pi/4 * ((D_o - 2/4*t_c)^2 - (D_o - 3/4*t_c)^2);
A_90_o = pi/4 * ((D_o - 3/4*t_c)^2 - (D_o - 4/4*t_c)^2);
A_90_i = pi/4 * ((D_o - 4/4*t_c)^2 - (D_o - 5/4*t_c)^2);
A_m45_i = pi/4 * ((D_o - 5/4*t_c)^2 - (D_o - 6/4*t_c)^2);
A_45_i = pi/4 * ((D_o - 6/4*t_c)^2 - (D_o - 7/4*t_c)^2);
A_0_i = pi/4 * ((D_o - 7/4*t_c)^2 - (D_o - 8/4*t_c)^2);
A_lam = [A_0_o;A_45_o;A_m45_o;A_90_o;A_90_i;A_m45_i;A_45_i;A_0_i]; %areas of the casing sections


%% calculating u1
S_lam = E_lam * A_lam;
x_1 = linspace(0,L,1000);
u1_x = (T .* cos(theta) ./ S_lam) .* (L - x_1);
figure(1)
plot(x_1, u1_x)
xlabel('x_1 [m]')
ylabel('u_1 / u_2 [m]')
title('Displacement u_1/u_2 along the Rocket')
grid on
hold on

%% H33 Calculations

D_lam = 2*linspace(1.735, 1.855, 9);
sum_t = 0;
for i=1:length(E_lam)
    sum = E_lam(i)*(D_lam(i+1)^4-D_lam(i)^4);
    sum_t = sum_t + sum;
end
h33 = sum_t * pi / 64;
```

```
%% calculating u2

u2_x = (P_2 ./ (24 .* h33)).*x_1.^4 + (T .* sin(theta) ./ (6 .* h33)).*x_1.^3 + ...
    (-1.* P_2 ./ (6 .* h33) .* L.^3 - (T .* sin(theta) .* L^2 ./ (2 .* h33))).*x_1 + ...
    (P_2 .* L.^4 / (8 .* h33)) + (T .* sin(theta) .* L.^3 ./ (3 .* h33)) + (P_2 .* L ./ k) + (T .* sin(theta) ./ k);
plot(x_1, u2_x)
legend('u_1','u_2')
hold off
```

```
%% calculating M3

m3_x = P_2 ./ 2 .* x_1.^2 + T .* sin(theta) .* x_1;
figure(2)
plot(x_1, m3_x)
xlabel('x_1 [m]')
ylabel('M_3 [Nm]')
title('Moment M_3 along the Rocket')
grid on
```

```
%% critical x1 position (5)

[m3_max, i] = max(m3_x);
x_cr = x_1(i);
```

```
%% axial stress distribution (6)

% propellant axial stress due to axial load
eps_1 = -1 * T * cos(theta) / S_lam;
sig_p_ax = eps_1 * E_p;
% bending stress
dummy_3 = D_lam(1) ./ 2 .* m3_max ./ h33;
sig_p_bend = -1 .* E_p .* dummy_3;

sig_p_u = sig_p_ax + sig_p_bend;
sig_p_l = sig_p_ax - sig_p_bend;

%axial stress due to axial load
for i=1:length(E_lam)
    sig_ax(i) = eps_1 .* E_lam(i);
end

%bending stress
dummy_1 = D_lam(2:9) ./ 2 .* m3_max ./ h33;
sig_bend_u = -1 .* E_lam .* dummy_1;
x_2_u = D_lam(2:9)/2;
sig_t_u = sig_bend_u + sig_ax;
```

```
figure(3)
hold on
stairs(sig_t_u, x_2_u,'b')
stairs(sig_t_l, x_2_l, 'b')
plot([sig_p_u, sig_p_u, sig_t_u(1)], [0,D_lam(1)/2,x_2_u(1)], 'b')
plot([sig_p_l, sig_p_l, sig_t_l(8)], [0,-D_lam(1)/2,x_2_l(8)], 'b')
xlabel('\sigma_{axial} [Pa]')
ylabel('x_2 [m]')
title('Stress Distribution in the Cross-section at x_{critical}')
grid on
hold off
```

```
figure(4)
hold on
stairs(sig_t_u, x_2_u,'b')
stairs(sig_t_l, x_2_l, 'b')
ylim([1.74 2])
xlim([-2*10^8 0])
xlabel('\sigma_{axial} [Pa]')
ylabel('x_2 [m]')
title('Top Stress Distribution in the Cross-section at x_{critical}')
grid on
hold off


figure(5)
hold on
stairs(sig_t_u, x_2_u,'b')
stairs(sig_t_l, x_2_l, 'b')
ylim([-2 -1.74])
xlim([0 inf])
xlabel('\sigma_{axial} [Pa]')
ylabel('x_2 [m]')
title('Bottom Stress Distribution in the Cross-section at x_{critical}')
grid on
hold off


%% section 7

adj_sig_u = sig_t_u .* 1.25 .* 1.15;
adj_sig_l = sig_t_l .* 1.25 .* 1.15;
```